



Epidermal growth factor receptor abnormalities in atypical teratoid/rhabdoid tumors and an unusual case with gene amplification

著者	Satomi Kaishi, Morishita Yukio, Murata Yoshihiko, Shiba-Ishii Aya, Sugano Masato, Noguchi Masayuki
journal or publication title	Pathology, research and practice
volume	209
number	8
page range	521-526
year	2013-08
権利	(C) 2013 Elsevier GmbH. NOTICE: this is the author 's version of a work that was accepted for publication in Pathology - Research and Practice. Changes resulting from the publishing process, such as peer review, editing, corrections, structural formatting, and other quality control mechanisms may not be reflected in this document. Changes may have been made to this work since it was submitted for publication. A definitive version was subsequently published in Pathology - Research and Practice, 209, 8, 2013, http://dx.doi.org/10.1016/j.prp.2013.06.007 .
URL	http://hdl.handle.net/2241/120753

doi: 10.1016/j.prp.2013.06.007

Epidermal growth factor receptor abnormalities in atypical teratoid / rhabdoid tumors and an unusual case with gene amplification

Kaishi Satomi, Yukio Morishita, Yoshihiko Murata, Aya Shiba-Ishii, Masato Sugano, Masayuki

Noguchi

K. Satomi, A. Shiba-Ishii, M. Sugano, M. Noguchi

Department of Diagnostic Pathology, Faculty of Medicine, University of Tsukuba, 1-1-1 Tennodai,

Tsukuba-shi, Ibaraki 305-8575, Japan

Y. Morishita

Department of Diagnostic Pathology, Tokyo Medical University Ibaraki Medical Center, 3-20-1

Chuo Ami-machi, Inashiki-gun, Ibaraki 305-0395, Japan

Y. Murata

Department of Diagnostic Pathology, Graduate School of Comprehensive Human Sciences,

University of Tsukuba, 1-1-1 Tennodai, Tsukuba-shi, Ibaraki 305-8575, Japan

All correspondence to K. Satomi, M.D., Department of Diagnostic Pathology, Faculty of Medicine,

University of Tsukuba, 1-1-1 Tennodai, Tsukuba-shi, Ibaraki 305-8575, Japan

E-mail: kaishis@md.tsukuba.ac.jp

Tel: +81-29-853-0263, Fax: +81-29-853-3150

Running title: EGFR abnormalities in AT/RT

Keywords

Amplification, Atypical teratoid/rhabdoid tumor, EGFR, Fluorescence in situ hybridization,

Immunohistochemistry

Summary

Atypical teratoid/rhabdoid tumor (AT/RT) is a rhabdoid tumor of the central nervous system comprising a mixture of small round cells and mesenchymal and/or epithelial elements, showing mutation of the *SMARCB1* gene or *SMARCA4* gene. The epidermal growth factor receptor (EGFR) is one of the tyrosine kinase receptors whose overexpressed protein plays important roles in the malignant characteristics of various tumors. We analyzed 8 Japanese cases of AT/RT for EGFR protein overexpression and *egfr* gene amplification using immunohistochemistry and fluorescence *in situ* hybridization. The patients included 7 boys and one girl (age range 13 days – 2 years), and the tumors were localized in the frontal lobe (1 case), lateral ventricle (1 case), third ventricle (1 case), fourth ventricle (3 cases), and cerebellum (2 cases). We found that all (100%) of them partially expressed a high level of EGFR protein, and that one case showed amplification of *egfr*, the amplified area being localized and limited to a specific area within the tumor. We speculate that AT/RT is a tumor with heterogeneous *egfr* amplification, and that the frequency of amplification may depend on loss of function of the specific chromatin-remodeling member.

Introduction

Rhabdoid tumor was originally described in 1978 as a primary malignant “rhabdomyosarcomatous variant” of Wilms’ tumor in the kidney [1]. In 1996, Rorke et al. first proposed a distinct entity: atypical teratoid/rhabdoid tumor (AT/RT) of the brain, comprising a mixture of rhabdoid tumor, a tumor with small round cells, and mesenchymal and/or epithelial elements [2]. Biegel et al. subsequently reported monosomy 22 or deletion of chromosome 22q11 as the primary cytogenetic change in AT/RT, and found that *SMARCB1* (*hSNF5/INI-1*) mutation was included in the affected region. Subsequently, *SMARCB1* mutation was also detected in cases of AT/RT without chromosomal abnormality of chromosome 22q11 [3, 4]. More recently, cases of AT/RT without *SMARCB1* mutation have also been reported. These tumors retained *SMARCB1* expression but had mutation of *SMARCA4*, which is another member of the SWI/SNF chromatin-remodeling complex [5]. Clinicopathologically, AT/RT of the central nervous system is an extremely aggressive tumor of early childhood. The current estimated incidence of AT/RT is 2–3% of all primary CNS tumors in children. When aggressive multidisciplinary therapies are adopted, the median survival period is 16.75 months and the median event-free survival is 10 months [6].

The epidermal growth factor receptor (EGFR) is one of the tyrosine kinase receptors, and overexpressed EGFR protein plays important roles in the malignant characteristics of various tumors. Among brain tumors, EGFR protein overexpression is detected in glioblastoma, and is usually associated with *egfr* amplification [7].

There have been conflicting reports concerning the status of EGFR protein expression and *egfr* amplification in AT/RT. Jeibmann et al. found neither *egfr* amplification nor EGFR overexpression in 9 cases of AT/RT [8], whereas Patereli et al. found that among 7 such cases, 3 were positive for EGFR expression [9].

In the present study, we investigated the EGFR status of AT/RT using immunohistochemistry (IHC) and fluorescence *in situ* hybridization (FISH) with serial formalin-fixed, paraffin-embedded sections of surgical specimens.

Materials and Methods

Cases

We analyzed 8 Japanese cases of AT/RT. The affected patients included 7 boys and one girl (age range 13 days – 2 years), and the tumors were localized in the frontal lobe (1 case), lateral ventricle (1 case), third ventricle (1 case), fourth ventricle (3 cases), and cerebellum (2 cases) (Table 1).

Immunohistochemistry

For immunohistochemical analysis, the following antibodies (clone) and their dilutions were used as primary antibodies: anti-EGFR (clone : 2-18C9, Dako Japan, Tokyo, Japan) 1:50, anti-EMA (E29, mouse monoclonal, Dako Japan) 1:100, anti-GFAP (rabbit polyclonal, Dako Japan) 1:100, anti-p53 (DO-7, mouse monoclonal, Dako Japan) 1:100, anti-synaptophysin (SY38, mouse monoclonal, Dako Japan) 1:50, anti-vimentin (V9, mouse monoclonal, Dako Japan) 1:200, anti-S-100 protein (rabbit polyclonal, Dako Japan) 1:500, anti-SMA (1A4, mouse monoclonal, Dako Japan) 1:200, anti-BAF47/INI-1 (25/BAF47, mouse monoclonal, BD, Nippon Becton Dickinson, Tokyo, Japan) 1:50, anti-Ki-67 (MIB-1, mouse monoclonal, Dako Japan), 1:100, anti-desmin (D33,

mouse monoclonal, Dako Japan), and anti-pankeratin (AE1/AE3 and PCK26, cocktail antibody, Ventana, Roche Tissue Diagnostics Japan, Tokyo, Japan).

All of the specimens had been previously fixed in 15% formalin and embedded in paraffin. Serial sections were cut at a thickness of 2 μ m, placed on slides, then deparaffinized in xylene and rehydrated in an ethanol series. The specimens were incubated with ChemMate POD Blocking Solution (Dako Japan) for 5 min at room temperature. After blocking, the sections were incubated with each primary antibody diluted in Dako REAL Antibody Diluent (Dako Japan) for 30 min at room temperature. Heat-mediated antigen retrieval was performed as follows: autoclaving for 15 min at 105°C: anti-EGFR, anti-p53, anti-synaptophysin, and anti-BAF47/INI-1; autoclaving for 10 min at 120°C: anti-GFAP, anti-vimentin, anti-SMA, anti-desmin, and anti-Ki-67. No antigen retrieval was performed for anti-EMA and anti-S-100 protein. The specimens were washed in Dako Wash Buffer and the EnVision[®] (Dako Japan) signal enhancement system was employed. These immunohistochemical processes were performed with histostainer (Nichirei Biosciences Inc., Tokyo, Japan) and the Ventana NexES[®] IHC staining system (Ventana, Roche Tissue Diagnostics Japan).

EGFR expression was scored in terms of intensity and the proportion of positive cells.

The stained specimens were evaluated by light microscopy, using a x10 objective. Only clear

staining of the tumor cell membranes was considered positive. Diffuse cytoplasmic or granular staining was diagnosed as negative. A semi-quantitative approach was used to generate a score for each tissue slide, as follows. The percentage of positive tumor cells was scored at intervals of 10% (0% to 100%). The dominant intensity pattern of staining was scored as: 1, negative or trace; 2, weak; 3, moderate; or 4, intense (Fig.1 A-D). The total score was calculated by multiplying the intensity score and the fraction score, producing a total range of 0–400. Specimens with low levels of expression were re-evaluated for the presence or absence of membranous or cytoplasmic staining using a x40 objective. Immunohistochemistry assays were evaluated by two independent pathologists (KS and YMo) who were blinded to the clinical data and the results of fluorescence *in situ* hybridization (FISH) to determine gene amplification, as described below. A consensus was reached for each slide after discussion of the results [10].

Fluorescence in situ hybridization (FISH)

Dual-color, dual-target FISH assays were performed using the LSITM EGFR Spectrum Orange/CEP7 Spectrum Green Probe (Vysis, Abbott Japan, Tokyo, Japan). 4'6-Diamidino-2-phenylindole (DAPI) (DAPI I, Vysis, Abbott Japan) was used for chromatin

counterstaining. All specimens had been previously fixed in 15% formalin and embedded in paraffin.

Sections 5 µm thick were deparaffinized, rehydrated, and immersed in 0.2 N HCl for 10 min, then

incubated in pretreatment solution (Vysis, Abbott Japan) for 30 min at 80°C, and digested with

protease solution for 30 min at room temperature. The sections were incubated in probe solution

(Vysis, Abbott Japan) at 73°C for 5 min to co-denature the EGFR and CEP7 probes, and left

overnight to hybridize at 37°C. Post-hybridization stringency washing was done in a water bath at

72°C for 4 min. After washing and wiping off the wash buffer, the sections were stained with DAPI

(Vysis, Abbott Japan) and then mounted under coverslips.

Analyses were performed using a fluorescence microscope (BZ-9000, Keyence Corp., Osaka,

Japan). The EGFR gene was visualised as a red signal using a Spectrum Orange filter, CEP7 as a

green signal using a fluorescein isothiocyanate filter, and nuclei as a blue signal using a DAPI filter.

Two independent pathologists (KS and YMo) scored at least 100 non-overlapping interphase nuclei

for the number of copies of EGFR and CEP7, and then a consensus about each slide was reached

after discussion. The observers were blinded to the clinical data and the results of

immunohistochemistry. EGFR status was scored as the number of EGFR signals per nucleus and as

the ratio of EGFR signals to CEP7 signals. Negative controls consisted of non-tumoral colorectal

mucosa contiguous with adenocarcinoma, which was the positive control for amplified EGFR. An

increased EGFR copy number was defined as the presence of three or more signals per nucleus.

Results

We analyzed 8 Japanese cases of AT/RT for EGFR protein overexpression and *egfr* gene amplification. These 8 cases were diagnosed as AT/RT according to the WHO Classification of Tumours of the Central Nervous System, fourth edition [11]. The 8 affected patients included seven boys and one girl (age range 13 days – 2 years), and the tumors were localized in the frontal lobe (1 case), lateral ventricle (1 case), third ventricle (1 case), fourth ventricle (3 cases), and cerebellum (2 cases) (Table 1). Although the sample set was small, the marked male predilection was noteworthy. There was no other evident trend in the patient profiles.

All 8 cases showed diagnostic morphological features such as rhabdoid cells and embracing cells (Fig.2 A-C). In addition, various phenotypes were confirmed using immunohistochemistry (data not shown). The tumors always focally expressed GFAP, synaptophysin, S-100 protein, SMA, cytokeratin (pankeratin), EMA, and vimentin. All of these cases were negative for desmin. Most of the tumor cells were positive for p53 in every case. Furthermore, all showed loss of nuclear expression of BAF47/INI1 in the tumor cells, whereas positive expression was confirmed in capillary endothelia as an internal control (Fig.2D).

All 8 cases (100%) expressed the EGFR protein (Table 1, Fig.3). The EGFR-positive

areas showed not only a diffuse pattern but also single-cell positivity. There were no correlations between the immunohistochemical scores and clinical features, or between EGFR-positive cells and any specific histological features. EGFR expression showed no association among histological features such as rhabdoid cells, embracing cells, epithelioid cells, spindle cells, papillary structures, adenomatous areas, or poorly differentiated ribbons and cords (data not shown).

Fluorescence *in situ* hybridization (FISH) analysis was performed to detect *egfr* amplification. Surprisingly, one case (case No.3 in Table 1, 1/8, 12.5%) showed focal *egfr* amplification (Table 1, Fig.4 A,B). The other seven cases showed no amplification in any of the microscopic fields examined. Case No.3, with an area of *egfr* amplification, showed relatively higher semi-quantitative immunohistochemical scores (Proportion: 40, Intensity: 4, Score: 160), but these were not the highest scores among the 8 cases. To clarify the association between the area of *egfr* amplification and the area of EGFR protein expression, we reviewed serial sections of FISH specimens using immunohistochemistry. The serial area of amplification showed strong heterogeneous EGFR positivity (intensity=4) and it extended to 40% of the specimen (Proportion =40) (Fig.4 C,D).

Discussion

The aim of this study was to assess EGFR protein overexpression and the frequency of *egfr* gene amplification in cases of AT/RT [8, 9]. We detected EGFR protein expression in all 8 cases of AT/RT examined, and one case showed *egfr* amplification. Interestingly, the area of *egfr* amplification was localized and limited in extent.

On the basis of our results, it seemed that EGFR expression and *egfr* amplification were not associated with each other, or with any cell type, despite intensive examination of many microscopic fields. However, the amount of specimens was admittedly small, and the clones of the antibodies or FISH probes used may have been responsible for the discrepancy between our results and those of previous studies.

Various solid tumors show high levels of EGFR protein overexpression. Since the EGFR is a tyrosine kinase receptor, its high expression is associated with oncogenesis or tumor progression. Anti-EGFR molecular targeted therapy is now widely accepted for patients with colon cancers. Amplification of *egfr* leads to overexpression of EGFR protein [13], and this is associated with poor prognosis; *egfr* amplification is also predictive of the efficacy of anti-EGFR agents in patients with colon cancer [14]. In breast cancer, however, amplification of *egfr* and overexpression of EGFR

protein are not always correlated. This may be due to epigenetic regulation, and microsatellite alterations in the regulating sequences of *egfr* have already been reported [15, 16].

Recently, Singh et al. reported that inhibition of the EGFR-ErbB2 signal pathway with lapatinib resulted in antitumor activity in AT/RT cell lines [12]. Although there are currently no clinical data for the use of lapatinib in AT/RT, this report showed that human AT/RT tumor cells are dependent on the EGFR-ErbB2 signal pathway, and that it would be a potentially useful therapeutic target in AT/RT. Since *INI1/hSNF5*, *SMARCB1*, and *SMARCA4* are core members of the adenosine triphosphate (ATP)-dependent SWI/SNF chromatin-remodeling complex, genetic alteration in any of them leads to chromatin instability. This may result in non-homogeneous or unusual *egfr* amplification in a tumor. Therefore, we speculate that AT/RT is a tumor with heterogeneous *egfr* amplification, and that the frequency of amplification may depend on the loss of function of the specific chromatin-remodeling member. Aberration of the chromatin modifier is also able to explain how EGFR expression and *egfr* amplification differ according to tumor area or among cells. That is, the *egfr* gene is thought not to be stabilized in individual tumor cells, and its level of amplification may thus differ, even within a small area (Fig.4A). Our immunohistochemical analysis of serial sections from case No.3 showed that EGFR-positive cells were not distributed

uniformly within a given area, thus supporting the above possibility.

In recent years, the Notch and EGFR pathways have been shown to regulate neural stem cells and neural progenitor cells [17]. The type of cell from which AT/RT originates is still under debate, and possible candidates include meningeal cells and germ cells. However, neural stem cells and neural progenitor cells have also been suggested, and it is possible that EGFR-positive cells interact with the Notch pathway and regulate neural stem/progenitor-like cells, thus acting as “tumor initiating cells”. The Notch-EGFR pathway or its member molecules may thus be promising new candidates for molecular targeted therapy.

Our present results support the possibility that AT/RT is a multi-phenotypic tumor with aberration of the chromatin modifier, and we speculate that it is an embryonal tumor in which neural stem cells or neural progenitor cells play an important role.

Conflict of interest

None of the authors have any potential conflicts of interest to declare.

Acknowledgment

We thank Junko Hirato MD, PhD, and Atsuko Nakazawa MD, PhD, for advice with pathological diagnosis.

References

- [1] J.B. Beckwith, N.F. Palmer, Histopathology and prognosis of Wilms' tumors: results from the First National Wilms' Tumor Study, *Cancer* 41 (1978) 1937-1948.
- [2] L.B. Rorke, R.J. Packer, J.A. Biegel, Central nervous system atypical teratoid/rhabdoid tumors of infancy and childhood: definition of an entity, *J. Neurosurg.* 85 (1996) 56-65.
- [3] J.A. Biegel, L.B. Rorke, R.J. Packer, B.S. Emanuel, Monosomy 22 in rhabdoid or atypical tumors of the brain, *J. Neurosurg.* 73 (1990) 710-714.
- [4] J.A. Biegel, C.S. Allen, K. Kawasaki, N. Shimizu, M.L. Budarf, C.J. Bell, Narrowing the critical region for a rhabdoid tumor locus in 22q11, *Genes Chromosomes Cancer* 16 (1996) 94-105.
- [5] M. Hasselblatt, S. Gesk, F. Oyen, S. Rossi, E. Viscardi, F. Giangaspero, C. Giannini, A.R. Judkins, M.C. Fruhwald, T. Obser, R. Schneppenheim, R. Siebert, W. Paulus, Nonsense mutation and inactivation of SMARCA4 (BRG1) in an atypical teratoid/rhabdoid tumor showing retained SMARCB1 (INI1) expression, *Am. J. Surg. Pathol.* 35 (2011) 933-935.
- [6] J.M. Hilden, S. Meerbaum, P. Burger, J. Finlay, A. Janss, B.W. Scheithauer, A.W. Walter, L.B. Rorke, J.A. Biegel, Central nervous system atypical teratoid/rhabdoid tumor: results of therapy in children enrolled in a registry, *J. Clin. Oncol.* 22 (2004) 2877-2884.

- [7] L.J. Layfield, C. Willmore, S. Tripp, C. Jones, R.L. Jensen, Epidermal growth factor receptor gene amplification and protein expression in glioblastoma multiforme: prognostic significance and relationship to other prognostic factors, *Appl. Immunohistochem. Mol. Morphol.* 14 (2006) 91-96.
- [8] A. Jeibmann, H. Buerger, M. Fruhwald, M. Hasselblatt, No evidence for epidermal growth factor receptor amplification and overexpression in atypical teratoid/rhabdoid tumors, *Acta Neuropathol.* 112 (2006) 513-514.
- [9] A. Patereli, G.A. Alexiou, K. Stefanaki, M. Moschovi, I. Doussis-Anagnostopoulou, N. Prodromou, O. Karentzou, Expression of epidermal growth factor receptor and HER-2 in pediatric embryonal brain tumors, *Pediatr. Neurosurg.* 46 (2010) 188-192.
- [10] F.R. Hirsch, M. Varella-Garcia, P.A. Bunn, Jr., M.V. Di Maria, R. Veve, R.M. Bremmes, A.E. Baron, C. Zeng, W.A. Franklin, Epidermal growth factor receptor in non-small-cell lung carcinomas: correlation between gene copy number and protein expression and impact on prognosis, *J. Clin. Oncol.* 21 (2003) 3798-3807.
- [11] David N. Louis, Hiroko Ohgaki, Otmar D. Wiestler, Webster K. Cavenee, WHO Classification of Tumours of the Central Nervous System, Fourth Edition, 2007, pp. 147-149.
- [12] A. Singh, X. Lun, A. Jayanthan, H. Obaid, Y. Ruan, D. Strother, S.N. Chi, A. Smith, P. Forsyth,

A. Narendran, Profiling pathway-specific novel therapeutics in preclinical assessment for central nervous system atypical teratoid rhabdoid tumors (CNS ATRT): Favorable activity of targeting EGFR- ErbB2 signaling with lapatinib, *Mol. Oncol.* 7 (2013) 497-512.

[13] A. Ooi, T. Takehana, X. Li, S. Suzuki, K. Kunitomo, H. Iino, H. Fujii, Y. Takeda, Y. Dobashi, Protein overexpression and gene amplification of HER-2 and EGFR in colorectal cancers: an immunohistochemical and fluorescent in situ hybridization study, *Mod. Pathol.* 17 (2004) 895-904.

[14] M. Moroni, S. Veronese, S. Benvenuti, G. Marrapese, A. Sartore-Bianchi, F. Di Nicolantonio, M. Gambacorta, S. Siena, A. Bardelli, Gene copy number for epidermal growth factor receptor (EGFR) and clinical response to anti-EGFR treatment in colorectal cancer: a cohort study, *Lancet Oncol.* 6 (2005) 279-286.

[15] N. Tidow, A. Boecker, H. Schmidt, K. Agelopoulos, W. Boecker, H. Buerger, B. Brandt, Distinct amplification of an untranslated regulatory sequence in the egfr gene contributes to early steps in breast cancer development, *Cancer Res.* 63 (2003) 1172-1178.

[16] H. Buerger, F. Gebhardt, H. Schmidt, A. Beckmann, K. Hutmacher, R. Simon, R. Lelle, W. Boecker, B. Brandt, Length and loss of heterozygosity of an intron 1 polymorphic sequence of egfr is related to cytogenetic alterations and epithelial growth factor receptor expression, *Cancer Res.* 60

(2000) 854-857.

[17] A. Aguirre, M.E. Rubio, V. Gallo, Notch and EGFR pathway interaction regulates neural stem cell number and self-renewal, *Nature* 467 (2010) 323-327.

Figure Legends

Fig.1 The intensity of immunohistochemical staining for EGFR.

The intensity was graded as: 1, negative or trace (A); 2, weak (B); 3, moderate (C); or 4, intense (D).

Scale bar is 50 μ m.

Fig.2 Histological features of atypical teratoid /rhabdoid tumors (AT/RTs).

A: In a low-power field, AT/RTs may contain areas that mimic other embryonal tumors such as

medulloblastoma or central nervous system primitive neuroectodermal tumor. The tumor is

composed of highly cellular, densely packed small round cells.

B: Rhabdoid cells are also a characteristic feature of AT/RTs. These cells have vesicular chromatin,

prominent nucleoli and eosinophilic globular cytoplasmic inclusions. Ultrastructurally, whorls of

intermediate filaments are evident.

C: Embracing cells are another characteristic feature of AT/RTs. These cells are sickle-shaped and

appear to embrace another tumor cell.

D: Immunohistochemical staining for expression of the INI-1/BAF47 protein is the most sensitive

and specific marker for AT/RTs. The expression of INI-1/BAF47 protein is lost in tumor nuclei, but

retained in the intratumoral endothelia.

Scale bar is 100 μm in A and D, 10 μm in B and C.

Fig.3 Immunohistochemical features of atypical teratoid /rhabdoid tumors.

A: HE, B: Immunohistochemistry for EGFR. The EGFR-positive cells appear to be localized in islands of tumor cells with clear cytoplasm. However, some other scattered tumor cells localized outside the islands are also positive.

Scale bar is 500 μm .

Fig.4 Dual color FISH assays using probes for EGFR (red) and chromosome 7 (CEP7, green) and immunohistochemistry of serial sections (case No.3).

A: Amplified area. Red signals represent amplification of the *egfr* gene (by more than 10-fold).

Green signals represent the centromere of chromosome 7, which contains the *egfr* gene.

B: Balanced disomic tumor cells. There is no *egfr* amplification.

C: An area with *egfr* amplification in a serial section. EGFR-positive cells and negative cells are admixed, and positive cells show strong positivity.

D: An area without *egfr* amplification in a serial section. There are scattered EGFR-positive cells,

but most of the tumor cells show no EGFR positivity.

Scale bar is 10 μm .

Table 1 Patient profiles, immunohistochemistry and gene amplification.

Case	Patient profile			Immunohistochemistry			FISH (EGFR/CEP7)
	Age	Sex	Tumor locus*	Proportion (0-100)	Intensity (1-4)	Score† (0-400)	
1	2 y.o.	M	Rt. LV	10	2	20	1.05
2	1 y.o.	M	4 th ventricle	30	4	120	0.97
3	2 y.o.	F	3 rd ventricle	40	4	160	>10‡
4	1 y.o.	M	4 th ventricle	20	4	80	1.04
5	13 days	M	cerebellum	30	3	90	1.10
6	2 y.o.	M	4 th ventricle	10	1	10	1.04
7	3 mo.	M	cerebellum	30	4	120	1.43
8	1 y.o.	M	Rt. FL	70	4	280	1.14

* LV: lateral ventricle, FL: frontal lobe

† The score was calculated by multiplying the proportion and the intensity, producing a total range of 0-400.

‡ Amplification

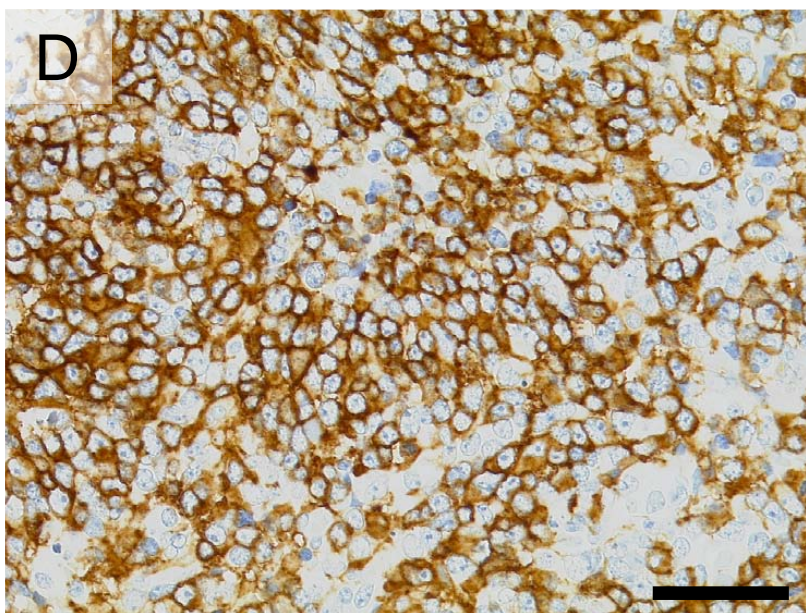
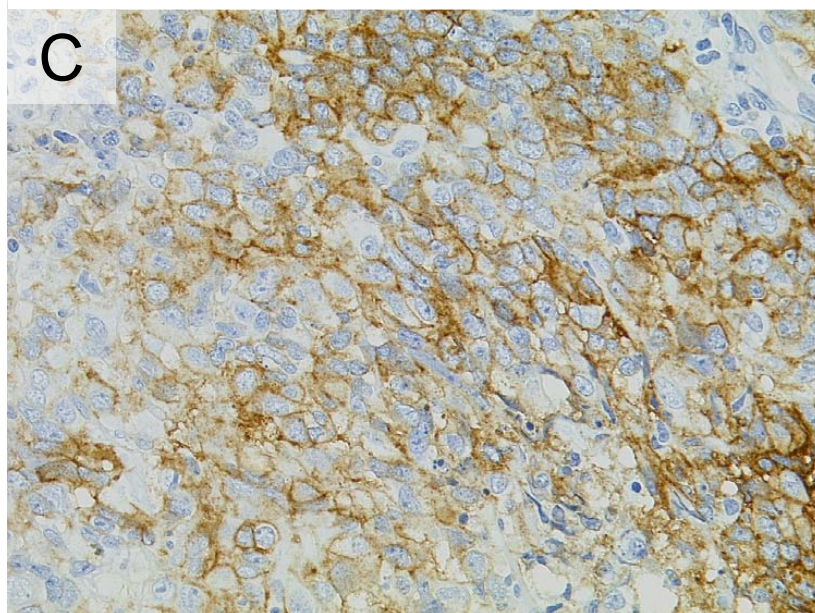
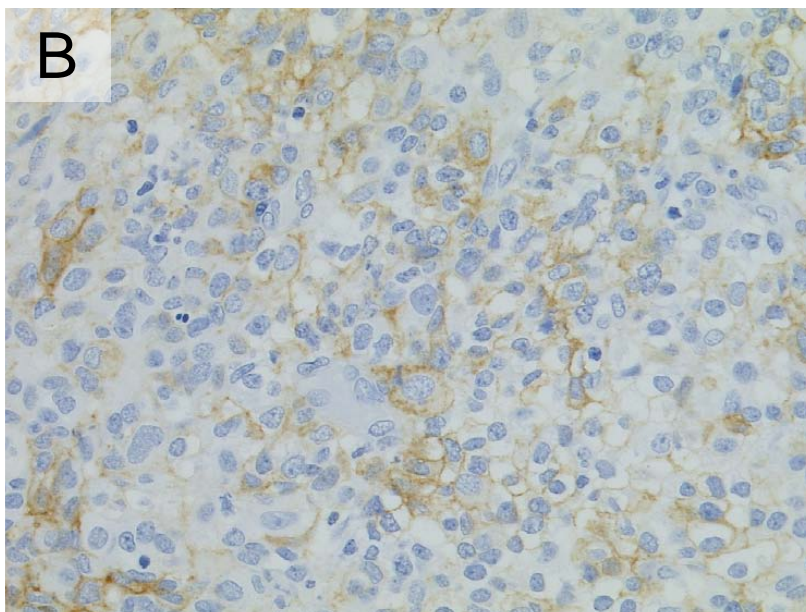
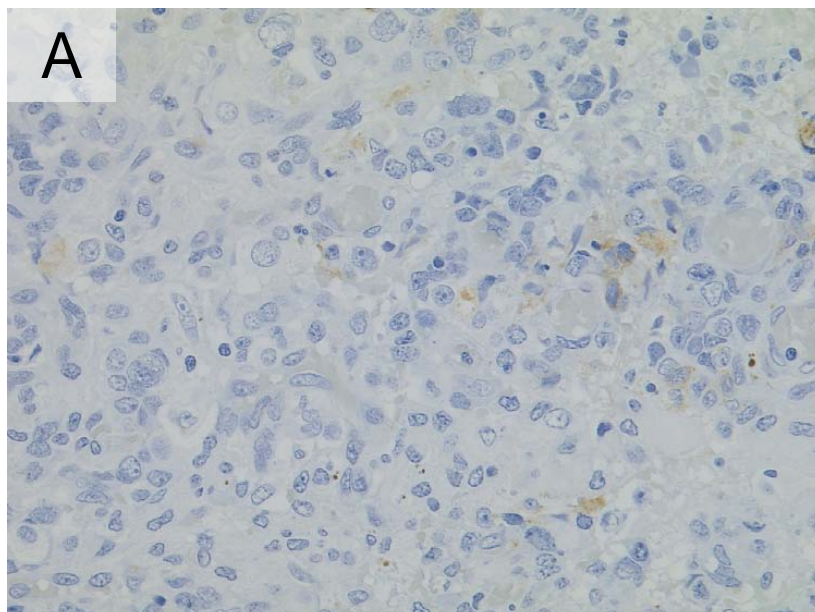


Fig.1

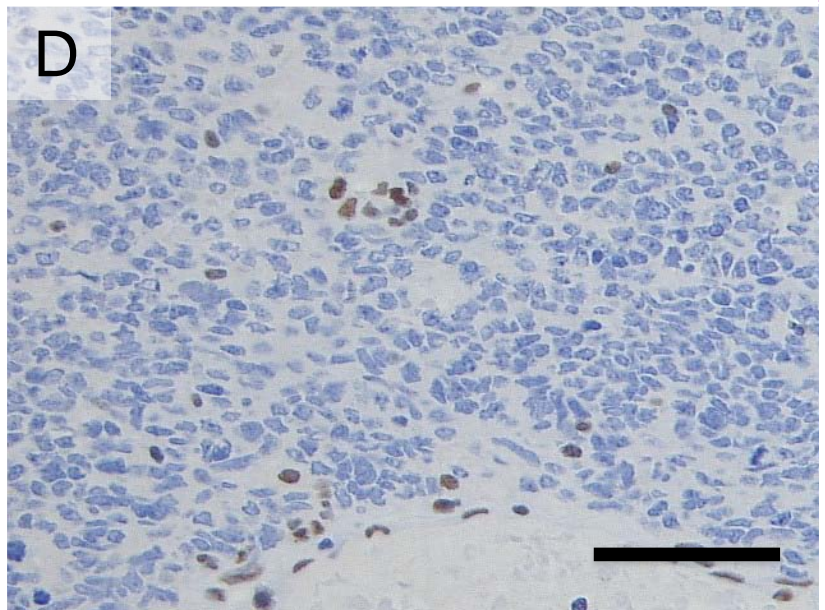
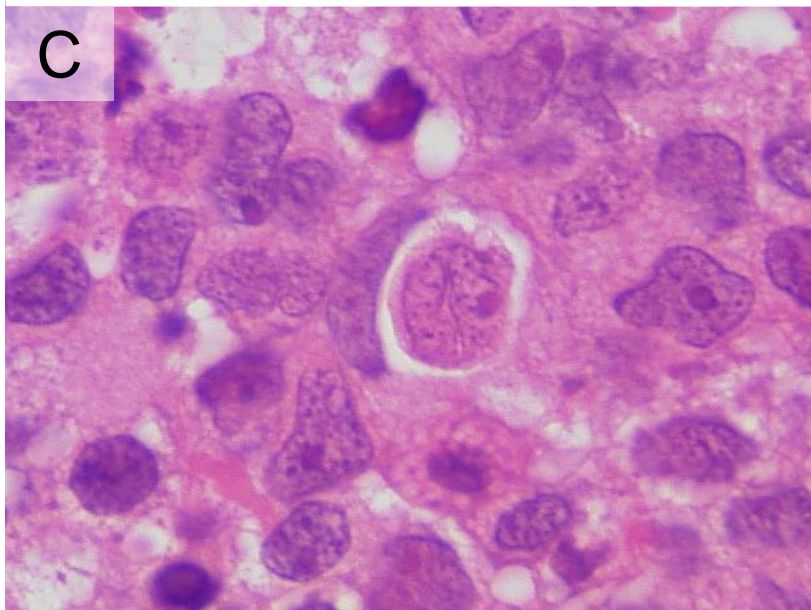
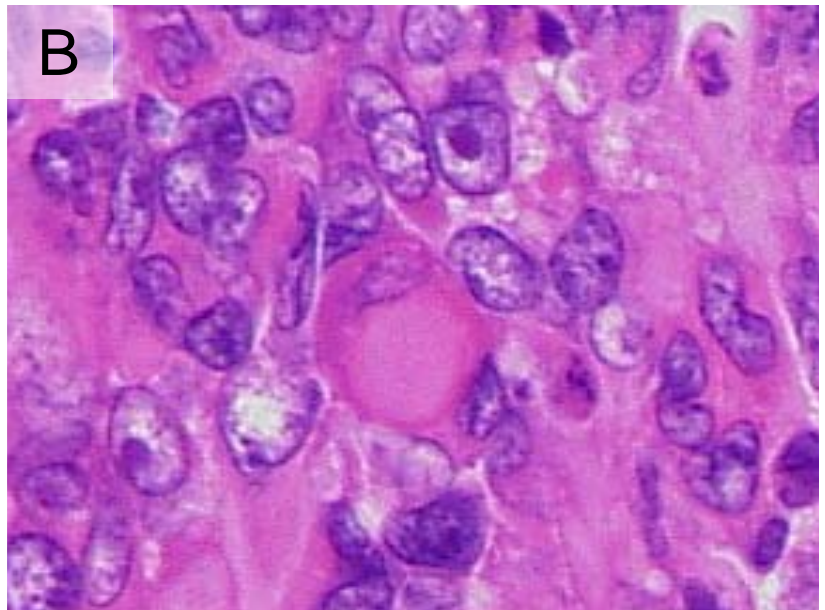
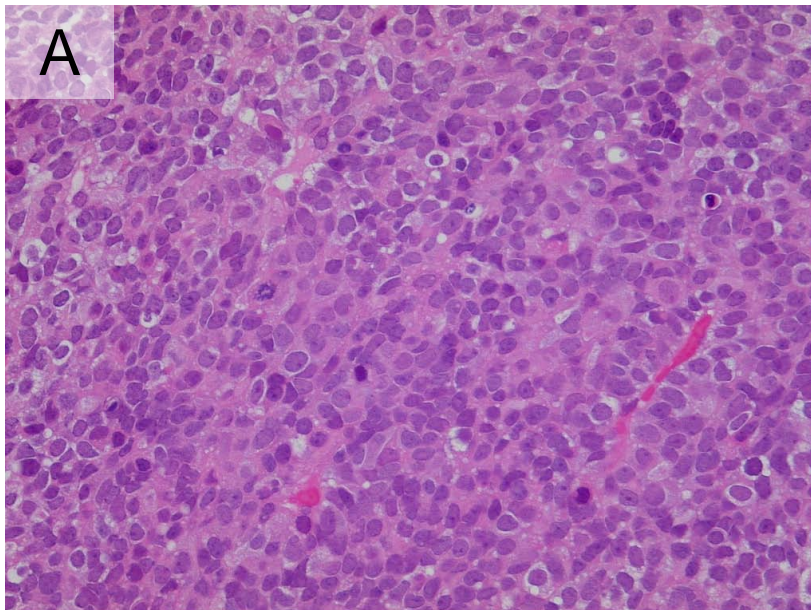


Fig.2

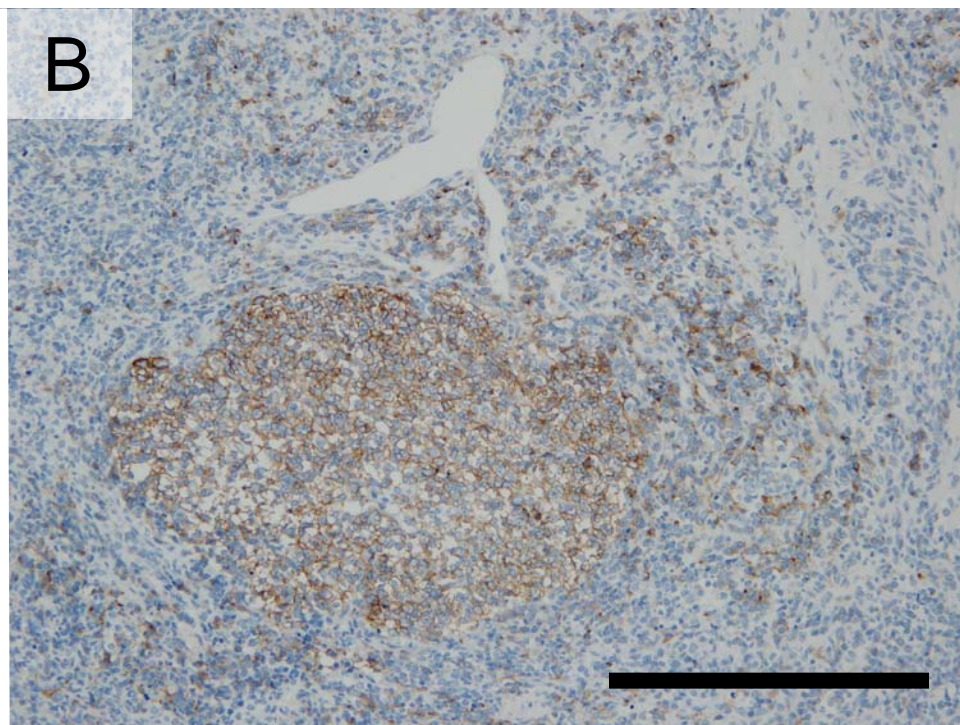
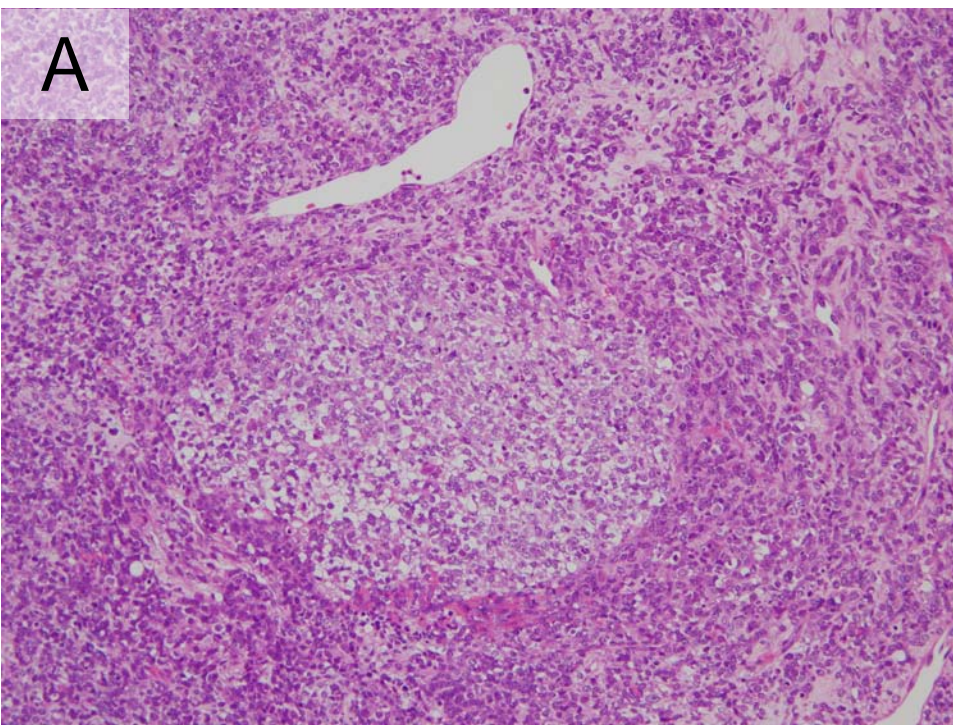


Fig.3

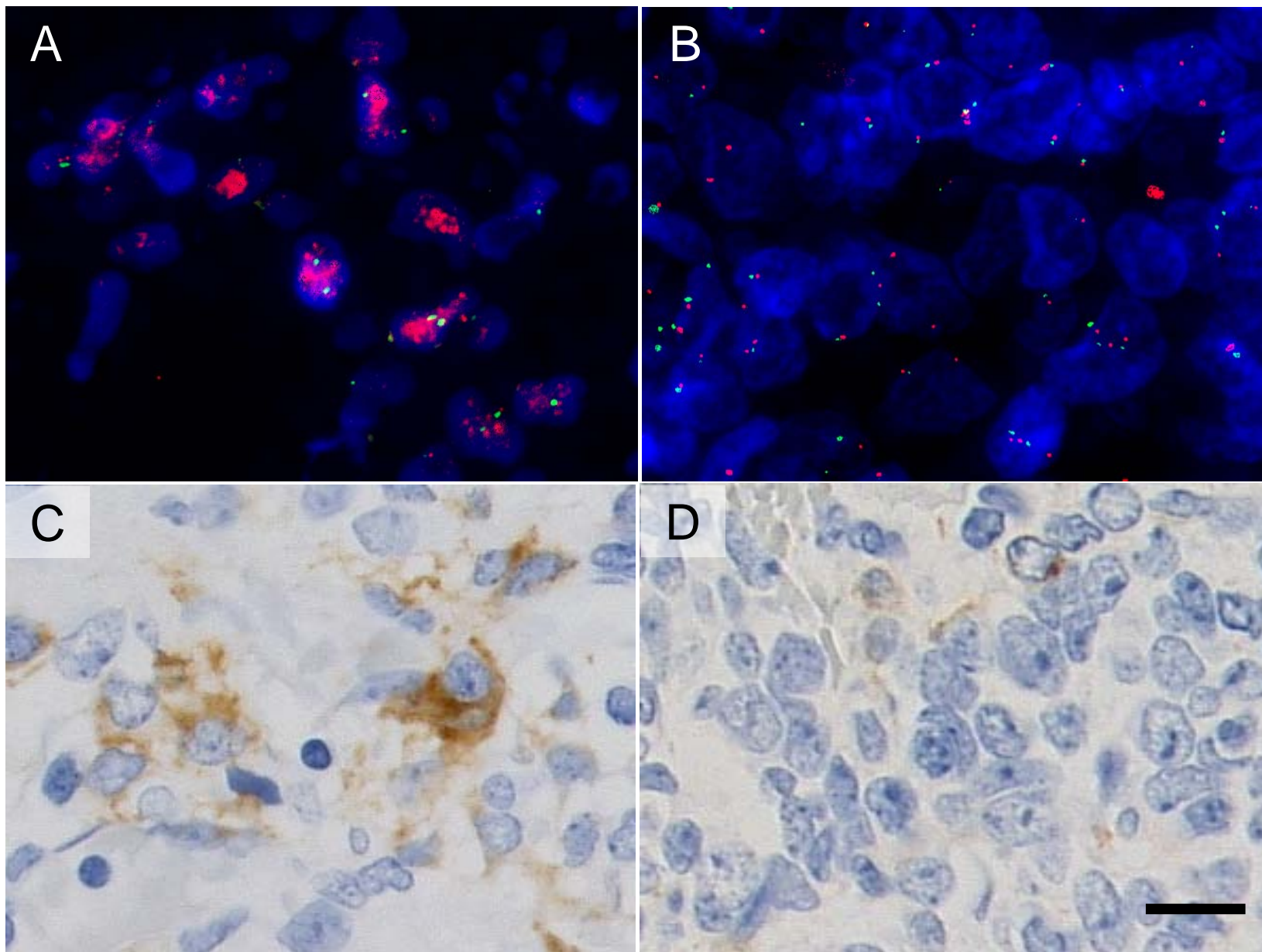


Fig.4